



## A conceptual NF/RO arrangement design in the pressure vessel for seawater desalination

Ali Altaee<sup>a,\*</sup>, Adel Sharif<sup>b</sup>

<sup>a</sup>Faculty of Engineering and Physical Science, University of the West of Scotland, Paisley PA1 2BE, UK

Tel. +447986517994; email: [ali.altaee@uws.ac.uk](mailto:ali.altaee@uws.ac.uk)

<sup>b</sup>Chemical & Process Engineering Department, University of Surrey, Guildford GU2 7XH, UK

Received 14 May 2013; Accepted 18 January 2014

---

### ABSTRACT

The main objective of this study is to understand the operation mechanisms of reverse osmosis (RO) membrane and optimization of the operating mechanisms of the RO system in order to reduce the membrane fouling and/or energy requirements. Typically, the high-pressure RO membrane vessel is loaded with membrane elements having the same flux and salt rejection rate. It has been conceived that when different types of RO elements are loaded into the pressure vessel in a special arrangement according to their permeability and salt rejection rate, this arrangement has the potential for reducing the energy consumption of the RO plant. Here, a conceptual design is introduced to describe this new idea. The effects of feed salinity and temperature were investigated in this paper using the reverse osmosis system analysis filmtec membrane design software. A two pass membrane treatment process was designed for desalting seawater at different salinities varied from 35,000 ppm to 43,000 ppm. The results showed a net energy saving from 2.5 to 3% (depends on the feed salinity) could be achieved. The effect of the feed temperature was also investigated, and the new design was found to be more energy efficient. Membrane scaling was also investigated in this study, and it was found that the new membrane arrangement design was less efficient than old design at feed salinity 35,000 ppm and vice versa at feed salinity 45,000 ppm. This was attributed to the use of high membranes permeabilities in the new design.

*Keywords:* Water and salt permeability; Reverse Osmosis; Pressure vessel design; Energy consumption

---

### 1. Introduction

Reverse osmosis (RO) seawater desalination is becoming a common trend for fresh water supply in large and small cities. As water scarcity problems intensify every day due to population growth and the degradation of freshwater quality, SWRO plants were

built around the world to provide potable water from seawater. The application of RO membranes were extended beyond seawater desalination to provide high-quality water to various pharmaceutical and food industries [1–4]. RO has an advantage over thermal desalination because of its lower energy requirements [1,5–11]. Nevertheless, the cost of RO is still considered high and can only be afforded by opulent and developed countries. Nowadays, most of the

---

\*Corresponding author.

desalination plants exist in the oil-rich Middle East countries, Europe and North America due to the high cost of desalted water. There are too many examples of successful RO plants for seawater desalination operating without major disruptions [6,10,12–14].

The RO membranes, however, require an intensive pre-treatment compared with the thermal technologies [15–19]. Furthermore, RO technology suffers from several drawbacks including scaling and biofouling. Antiscalants and various chemical compounds were used for fouling control in the RO system [6,12,20]. Previous studies showed that biofouling problem is more serious than scaling, although the latter cause serious damage to the RO membranes. It usually leads to a flux reduction and higher maintenance and operation cost [12,17,19]. Typically, predetermined dose of anti-scalants is added to the feed stream in order to prevent scaling elements precipitation in RO membranes. Some studies suggested using NF membranes as a pre-treatment for RO to reduce scaling problems [1,12,19]. Several pilot plants studied the feasibility of using the NF pre-treatment for the removal of divalent ions from RO feed. However, NF pre-treatment seems to be far from commercialization probably due to its high operation cost. Other researchers studied the potential of decreasing RO cost by using high permeability RO membranes or through optimization the number of RO elements in the pressure vessel [12,21,22].

In the current paper, a theoretical study was introduced to describe the effects of using RO elements of different permeabilities in the pressure vessel on the power consumption and the membrane performance. The reverse osmosis system analysis (ROSA) software was used throughout this study to simulate the RO membrane performance under different environment conditions. Filmtec brackish water reverse osmosis (BWRO) and seawater reverse osmosis (SWRO) membranes of different permeabilities were investigated in this study. The effect of seawater TDS and temperature were studied as well as the impacts of these parameters on the membrane performance. Filmtec BWRO and SWRO membranes of different permeabilities were investigated in this study. Effects of seawater TDS, temperature and the impacts of these parameters on the membrane performance were studied. Different feed salinities ranged from 35,000 to 45,000 mg/L were used in this study. For simplicity, apart from the scale analysis study, the composition of seawater was considered to be Na and Cl ions only. A scale analysis study was conducted to investigate the scale potential of both conventional (old) design and the proposed new design of RO membrane arrangement in the pressure vessel.

## 2. Theory

From the solution–diffusion theory, salt and water are diffused through the semi-permeable membrane according to the following equations:

$$J = A_w(\Delta P - \sigma \Delta \Pi) \quad (1)$$

$$J_s = B(\Delta C) \quad (2)$$

Where  $J$  is water flux through RO membrane ( $L/m^2 h$ ),  $A_w$  is membrane permeability coefficient ( $L/m^2 h \text{ bar}$ ),  $\Delta P$  is pressure difference across the membrane ( $\text{bar}$ ), and

$\sigma$  is membrane reflection coefficient. Membrane selectivity increases as  $\sigma$  approaches unity, for the RO membranes  $\sigma < 1$  but for simplicity a unit reflection coefficient is taken here.  $\Delta$  is the osmotic pressure of solute ( $\text{bar}$ ),  $J_s$  is salt flux ( $\text{kgm}^2/\text{h}$ ),  $B$  is salt diffusion coefficient ( $\text{m/d}$ ), and  $\Delta C$  is the difference of salt concentration across the membrane ( $\text{mg/L}$ ). Ideally,  $\Delta C$  is the difference between salt concentrations at the membrane surface and the permeate side of the membrane. But due to the difficulties to measure salt concentrations at the membrane surface, the concentration of bulk solution is often taken. The net driving pressure in RO membranes is the difference between hydraulic and osmotic pressure. The feed osmotic pressure increases with increasing the concentration of solute. Osmotic pressure can be calculated from the following Vant's Hoff equation:

$$\Pi = nCRT \quad (3)$$

Where  $C$  is the solute molar concentration,  $R$  is gas constant,  $T$  is temperature in Kelvin, and  $n$  is number of ions. As shown in Eq. (3), osmotic pressure is a function of solute concentration, type of solute and temperature. Since seawater is mainly NaCl, the effect of NaCl concentration on the performance of RO membrane was investigated in this study. The effect of seawater temperature variation on the performance of RO was also investigated. Water and salt diffusions in the RO membranes are affected by temperature; 3–5% flux increase per degree centigrade was reported [23].

Commercial SWRO and BWRO membranes have different water and salt permeabilities depending on the membrane applications. Typically, BWRO membranes are more permeable than SWRO membranes, but they have a lower salt rejection rate. In this study, different SWRO and BWRO membranes were investigated in an attempt to optimize the design of element arrangements

into the high-pressure vessel in a two pass RO desalination plant. The water and salt permeabilities of different types of RO membranes are listed in Table 1.

It is worth mentioning here that salt diffusion coefficient is calculated from the following equation:

$$B = (1 - R)J/R \tag{4}$$

Where *R* is the membrane salt rejection rate to sodium chloride. The value of *R* varies from 99.8 to 99% in SWRO and BWRO membrane, respectively. The higher *R* is the better salt rejection of the membrane. From A and B values (Table 1), SWRO membrane SW30HRLE-400i has a higher salt rejection rate and lower water permeability than SW30XLE-400i. This is probably due to the tight structure of SW30HRLE membrane. Similarly, Filmtec BW30-400 has higher salt rejection and lower water permeability than BW30LE-440 due to the tight structure of the membrane element.

In two pass membrane desalination, SWRO membranes are used in pass 1 followed by low-pressure BWRO membranes in pass 2. A schematic diagram of a SWRO-BWRO process is described in Fig. 1. A portion of pass 1 permeate is usually blended with a pass 2 permeate as required. While pass 2 concentrate is recycled back and mixed up with the pass 1 feed. Two different cases were investigated in this paper, and in case, one the same SWRO/BWRO membranes were loaded into the RO/BW pressure vessel as described in Fig. 2. In the second case, two different types of SWRO membranes were loaded into the pressure vessel with SWRO elements of higher permeability at the end (Fig. 2). As shown in Fig. 1, three pressure vessels of seven elements each were used in pass one to produce enough permeate feed to pass 2 in which one pressure vessel of seven elements was used.

Both salinity and temperature of seawater were investigated in this study. Different seawater temperatures ranged from 15 to 35°C were investigated then

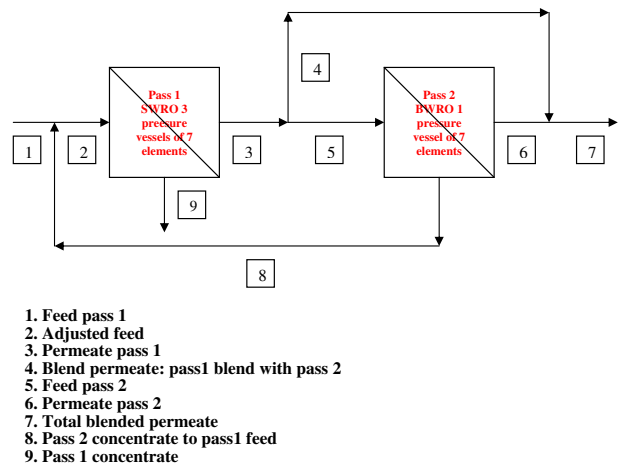


Fig. 1. Two passes SWRO and BWRO desalination process.

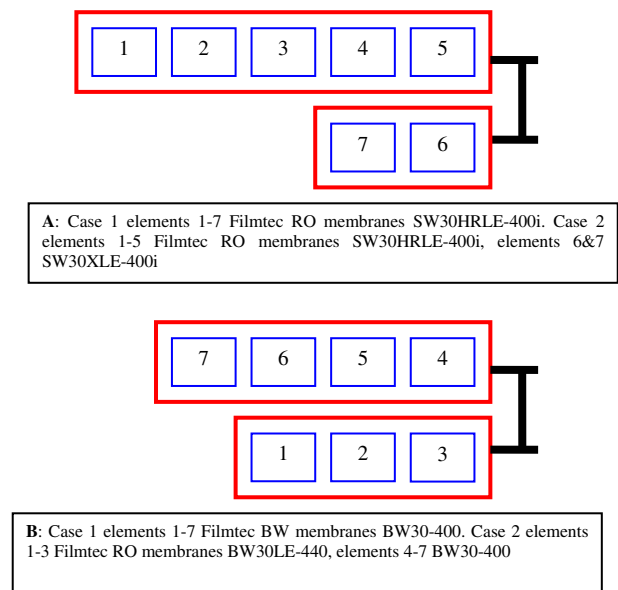


Fig. 2. SWRO and BWRO membrane arrangement in the pressure vessel.

Table 1  
Characteristics of Filmtec membranes

Filmtec membrane	Area (m <sup>2</sup> )	%Re	A <sub>w</sub> (L/m <sup>2</sup> h bar)	B (m/d)	Testing condition
SW30HRLE-400i	37	0.9975	1.056	0.00189	32,000 ppm NaCl, 5 ppm boron, 55 bar, pH 8, 25 C and 8% recovery
SW30XLE-400i	37	0.997	1.28	0.00276	32,000 ppm NaCl, 5 ppm boron, 55 bar, pH 8, 25 C and 8% recovery
BW30-400	37	0.995	3.14	0.00543	2000 ppm NaCl, 15.5 bar, pH 8, 25 C and 15% recovery
BW30LE-440	41	0.99	5.32	0.0108	2000 ppm NaCl, 10 bar, pH 8, 25 C and 15% recovery

seawater temperature fixed at 25 °C and different salinities from 35,000 to 43,000 ppm were investigated (Table 2). The TDS of permeate from Cases 1 and 2 should be identical or at least very close. The testing procedure of Cases 1 and 2 is described in Table 2. As mentioned before, ROSA software version 6.1 was used in this study to simulate the performance of SWRO and BWRO Filmtec membranes.

The performance of SWRO and BWRO membranes were predicted by ROSA 6.1 software. Case 1 represents the conventional design in which a similar type of membrane element was used in the pressure vessel, while in Case 2, two different types of membrane elements were used in the pressure vessel. In Case 2, five elements SW30HRLE-400i were placed in the lead position followed by two elements SW30XLE-400i which had higher permeability and slightly lower salt rejection rate than SW30HRLE-400i. In concept, this will, to some extent, reduce the power requirements of desalination. The BWRO membrane vessel, however, had a slightly different design in which the low permeability and salt rejection elements BW30-400 were placed in the tail position and BW30LE-440 elements were placed in the lead position. This arrangement is more efficient as the maximum recovery rate per elements will not be exceeded and permeate TDS will be lower.

### 3. Optimization number of RO elements in pressure vessel

It is very important to optimize the number of each type of RO and BW elements in the passes 1 and 2 pressure vessels. The approach used here was as follows:

- (1) Design two passes conventional SWRO-BWRO system in which the same membrane elements were used in each pressure vessel.
- (2) Design two passes SWRO-BWRO system in which two types of SWRO were used in pass 1, while the same BWRO membranes were used in pass 2. The specific power consumption ( $E_s$ ) and permeate TDS of each case was recorded and compared with the conventional design. In this step, the number of each type of RO membranes will be optimized and determined.
- (3) Design 2 pass SWRO-BWRO system in which the type and number of SWRO membranes were fixed from step 2 but two different types of BWRO membranes were used in pass 2. A number of case studies were investigated. The  $E_s$  and permeate TDS values of each case study were compared with the conventional design. At the end of step 3, the number of each type of BWRO was determined.

Table 2  
Testing condition for Cases 1 and 2

Design	Salinity (ppm)	Pf 1st pass (bar)	Pf 2nd pass (bar)	Temp. (°C)	SWRO membranes <sup>a</sup>	BWRO membranes
Case 1	41,000	70.77	18.22	15	7 elements SW30HRLE-400i	7 elements BW30-400
	41,000	68.99	14.66	20		
	41,000	67.86	12.06	25		
	41,000	66.92	10.14	30		
	41,000	66.36	8.8	35		
	35,000	58.02	11.97	25	7 elements SW30HRLE-400i	7 elements BW30-400
	37,000	61.2	12	25		
	39,000	64.2	12.03	25		
	41,000	67.84	12.06	25		
	43,000	71.34	12.09	25		
Case 2	41,000	69.66	12.1	15	5 elements SW30HRLE-400i & 2 elements SW30XLE-400i	3 elements BW30LE-440 & 4 elements BW30-400
	41,000	68.05	9.96	20		
	41,000	67.07	8.4	25		
	41,000	66.05	7.28	30		
	41,000	65.18	6.52	35		
	35,000	57.07	8.3	25	5 elements SW30HRLE-400i & 2 elements SW30XLE-400i	3 elements BW30LE-440 & 4 elements BW30-400
	37,000	60.18	8.33	25		
	39,000	63.37	8.37	25		
	41,000	66.66	8.4	25		
	43,000	70.07	8.34	25		

<sup>a</sup>Recovery rate in 1st pass is 50% and 2nd pass is 75%.

Results from ROSA showed an increase in the permeate TDS with increasing the number of SW30XLE-400i elements in the pressure vessel. When two SW30XLE-400i elements were placed into the tail position of the pressure vessel, the permeate TDS was slightly lower than in the conventional SWRO (Fig. 3). If the number of SW30XLE-400i increased to three elements, the permeate TDS increased higher than in the conventional system. Therefore, two SW30XLE-400i elements were used in pass 1. The  $E_s$  decreased linearly with increasing the number of SW30XLE-400i elements but that was at the cost of permeates TDS (Fig. 4). However, the results showed that the  $E_s$  in pass 2 was not affected significantly by the number of SW30XLE-400i in pass 1 (Fig. 5). But there was a slight increase in the pass 2  $E_s$  when the number of SW30XLE-400i membranes increased over five elements. Based on these results, two elements SW30XLE-400i and five elements SW30HRLE-400i were used in the pass 1 SWRO pressure vessel.

Step 3 was followed to optimize the number of BWRO in pass 2. As shown in Fig. 6, the permeate TDS increased with increasing the number of BW30LE-440 in the pressure vessel. For instance, when the number of BW30LE-440 elements increased to 5, the permeate TDS was 69.43 ppm; this was slightly higher than the permeate TDS in the conventional design system in which same type of elements were used in the pressure vessel. On the other hand, results showed a continuous drop in the specific power consumption with increasing the number of BW30LE-440 in the pressure vessel. In general, the permeate TDS tended to increase when the number of BW30LE-440 increased. From Figs. 6 and 7, and to be on the safe

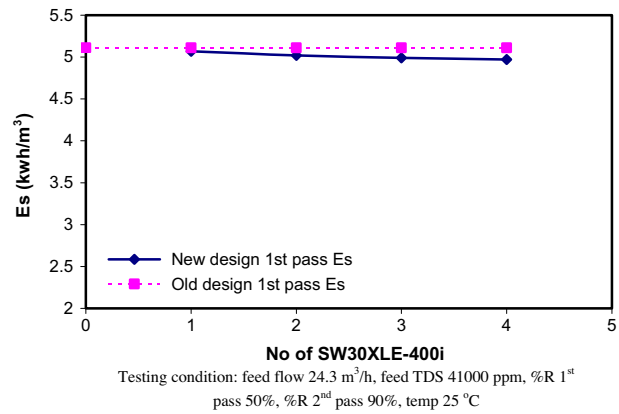


Fig. 4. Effect of SWRO elements number on the  $E_s$ .

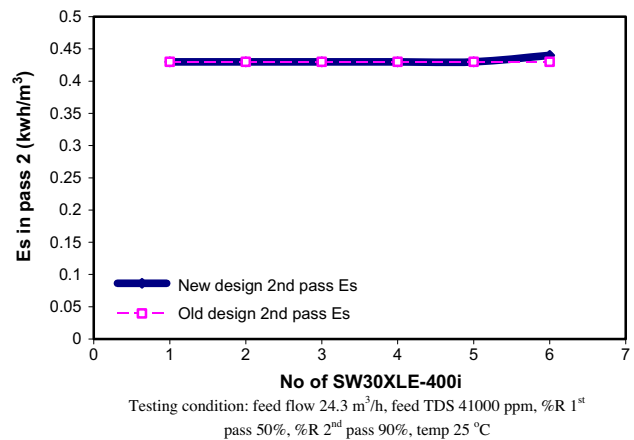


Fig. 5. Effects of SWRO element number on the  $E_s$  of second pass BWRO membranes.

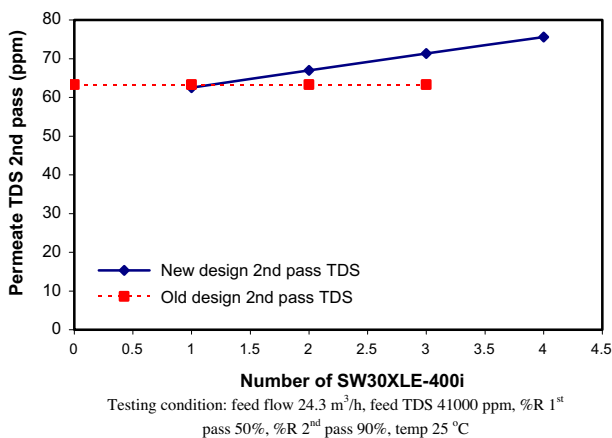


Fig. 3. Effect SWRO elements number on the permeate TDS.

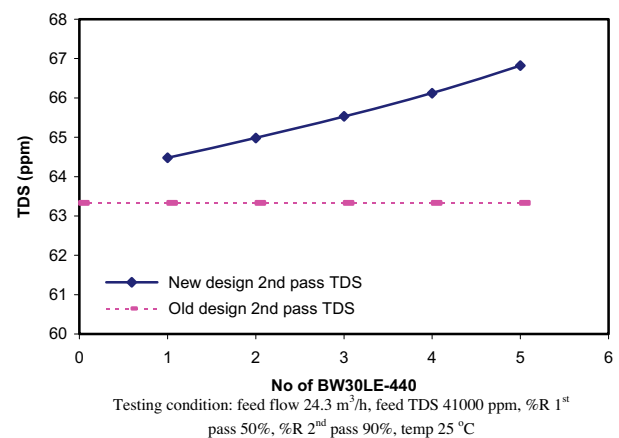


Fig. 6. Effect of BW30LE-440 elements number on the permeate TDS.

side, three BW30LE-440 and four BW30-400 elements were used in the pass 2 pressure vessel.

**4. Position of BWRO elements in the second pass vessel**

Two different types of BWRO membranes were used in the second pass BWRO membrane vessel; BW30-400 and BW30LE-440. The latter is a loose structure membrane and has relatively more water and salt permeabilities than the former membrane. Two scenarios were considered in this study; first using three elements BW30LE-440 in the lead followed by four elements BW30-400. Secondly, use four elements BW30-400 in the lead followed by three elements BW30LE-440. A range of feed water salinities between 35,000 ppm and 43,000 ppm were tested. The permeate TDS and energy consumption values were recorded for each case (Figs. 8–10). The results from ROSA showed insignificant difference in the permeate TDS and specific energy when BW30LE-440 was used in the lead or tail position, although there was a subtle advantage in favour of using BW30LE-440 in the lead position (Figs. 8 and 9). The reason for that was probably due to the higher feed pressure required at the beginning of pass 2 BWRO process (Fig. 10).

The simulation results showed that the overall recovery rate of each element in the pass 2 is more evenly distributed when the high permeability membrane was used in the lead position (Fig. 11). For this reason, three elements BW30LE-440 followed by four elements BW30-400 arrangement was used in this study.

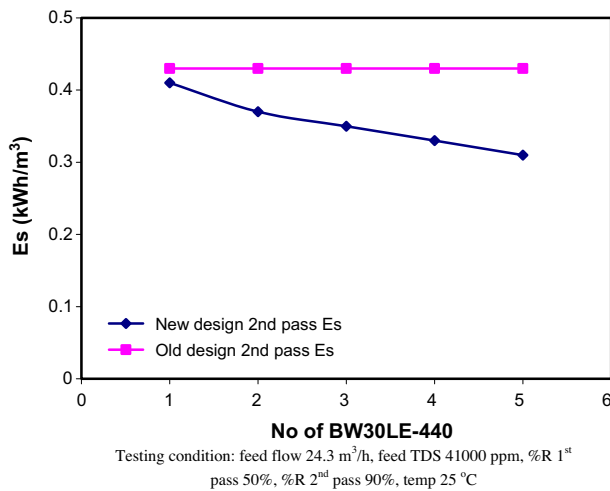


Fig. 7. Effect of BW30LE-440 elements number on the permeate TDS.

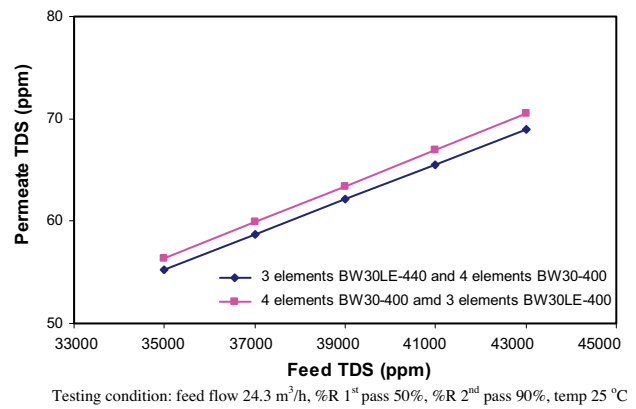


Fig. 8. Effect of the membrane position on the permeate concentration.

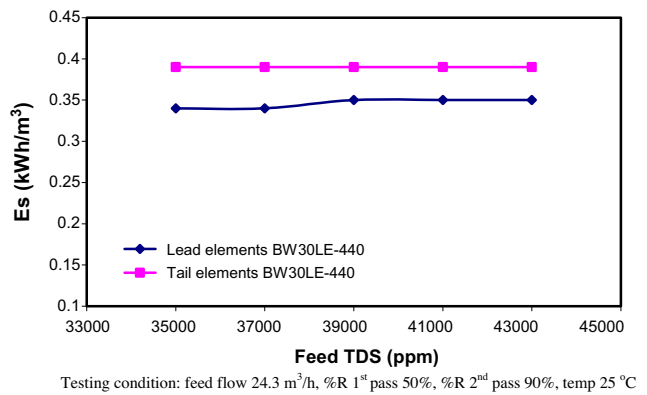


Fig. 9. Effect of the membrane position on the energy consumption.

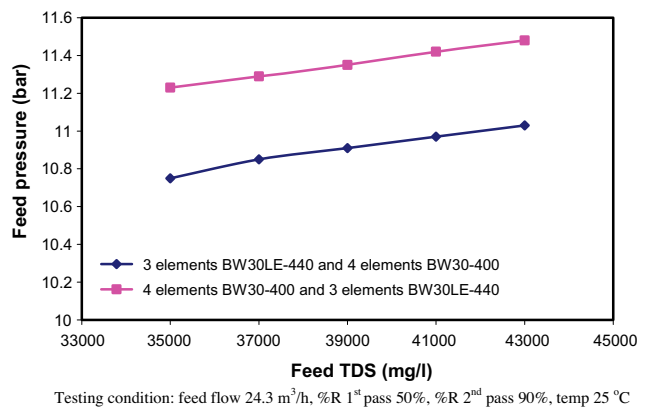


Fig. 10. Feed pressure in second pass BWRO desalination.

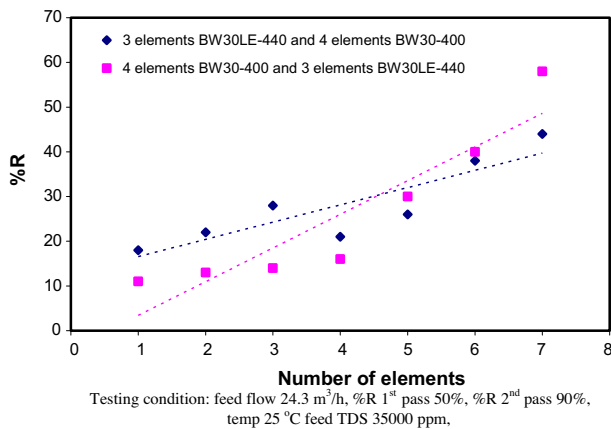


Fig. 11. Recovery rates of each element in second stage BWRO desalination.

## 5. Results and discussion

Two case studies were investigated in this paper; in Case 1, different membrane elements were used, while in Case 2, the same membrane elements were used. Each Cases 1 and 2 has 10 experiments (Table 2); experiments 1.1–1.5 investigated the variation of feed

temperature and experiments 1.6–1.10 the effect of feed salinity on the RO performance (Table 3).

The effects of feed water salinity and temperature on the permeate quality and energy consumption were investigated to compare the differences between the old and new design. As shown in Table 1, different feed water temperatures were investigated to cover the climatic change in feed temperature throughout the year. The effect of feed temperature increase on the pass 1 SWRO performance is shown in Fig. 12. The energy consumption in the conventional design was slightly higher than in the new design; this was because of the tighter structure of the SWRO membranes used in the conventional design and the higher feed pressure required in the conventional design (Fig. 13). A similar observation was noticed in the pass 2 BWRO membrane in which the energy consumption of the conventional design was higher than in the new design (Fig. 14). In the latter design, a loose structure membrane, BW30LE-440, was used. The overall power consumption in the conventional and new designs showed that the new design was slightly more energy efficient than the old design (Fig. 15). It was found that the total energy saving was slightly higher at low feed temperatures. This was due to the high membrane permeability at high feed temperatures. Up to

Table 3  
Operating condition for simulation tests

Test no <sup>a</sup>	Feed temp. (°C)	Feed salinity (mg/L)	Pass 1			Pass 2		
			Pf (bar)	Feed Π (bar)	Es (kWm <sup>3</sup> /h)	Pf (bar)	Feed Π (bar)	Es (kWm <sup>3</sup> /h)
1.1	15	41,000	69.66	28.34	4.89	12.1	0.13	0.45
1.2	20	41,000	68.05	28.97	4.8	9.96	0.19	0.37
1.3	25	41,000	67.07	29.24	4.7	8.4	0.26	0.32
1.4	30	41,000	66.03	29.84	4.64	7.28	0.37	0.28
1.5	35	41,000	65.18	30.11	4.56	6.52	0.51	0.26
1.6	25	35,000	57.07	24.55	3.99	8.3	0.22	0.32
1.7	25	37,000	60.18	25.97	4.21	8.33	0.23	0.32
1.8	25	39,000	63.37	27.41	4.43	8.37	0.24	0.33
1.9	25	41,000	66.66	28.86	4.66	8.4	0.25	0.33
1.10	25	43,000	70.07	30.32	4.9	8.43	0.27	0.33
2.1	15	41,000	70.77	28.01	4.96	18.22	0.11	0.55
2.2	20	41,000	68.99	28.61	4.85	14.66	0.16	0.45
2.3	25	41,000	67.86	29.16	4.75	12.06	0.23	0.38
2.4	30	41,000	66.92	29.76	4.69	10.14	0.32	0.32
2.5	35	41,000	66.36	30.35	4.64	8.8	0.46	0.29
2.6	25	35,000	58.02	24.76	4.04	11.97	0.19	0.39
2.7	25	37,000	61.2	26.21	4.26	12	0.21	0.39
2.8	25	39,000	64.45	27.67	4.49	12.03	0.22	0.39
2.9	25	41,000	67.84	29.13	4.72	12.06	0.23	0.4
2.10	25	43,000	71.34	30.60	4.96	12.09	0.24	0.4

<sup>a</sup>Recovery rate in 1st pass is 50% and 2nd pass is 75%, feed flow rate 24.3 m<sup>3</sup>/h (±0.2). Type and arrangement of SWRO and BWRO membrane elements is as shown in Fig. 2.

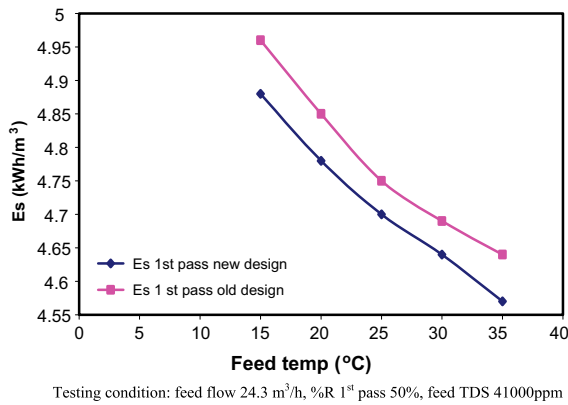


Fig. 12. Effect of feed temperature on 1st pass SWRO energy consumption.

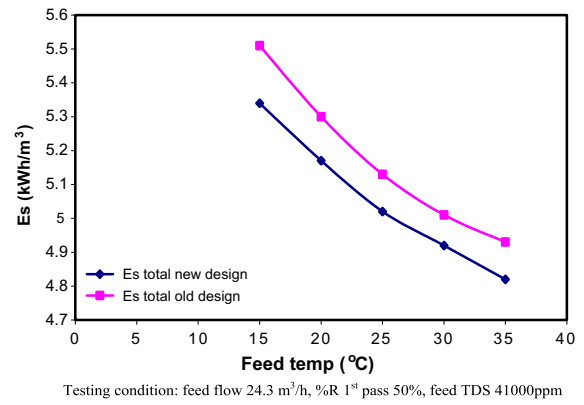


Fig. 15. Effect of feed temperature on the overall energy consumption.

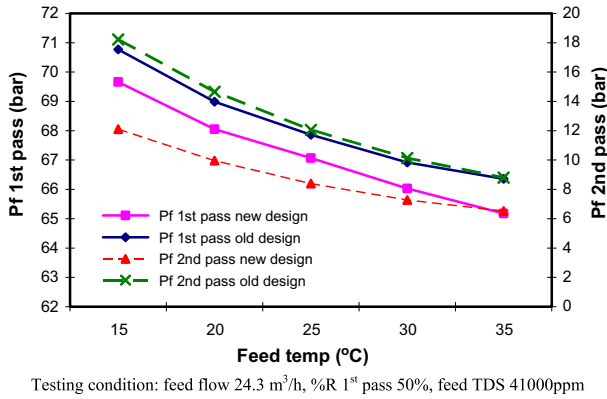


Fig. 13. Feed pressure variations with feed temperature.

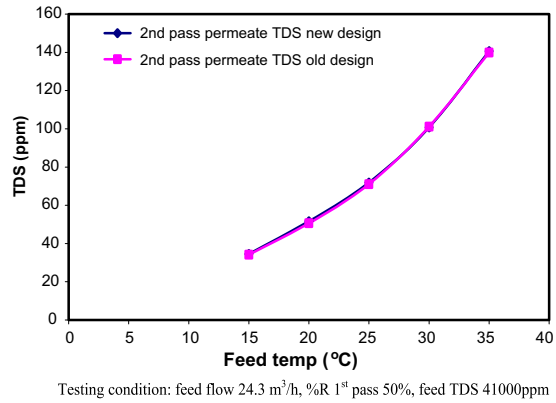


Fig. 16. Permeate TDS for the conventional and new designs at different feed temperatures.

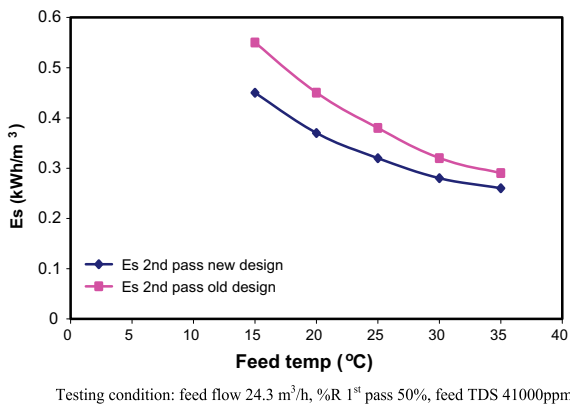


Fig. 14. Effect of feed temperature on 2nd pass BWRO energy consumption.

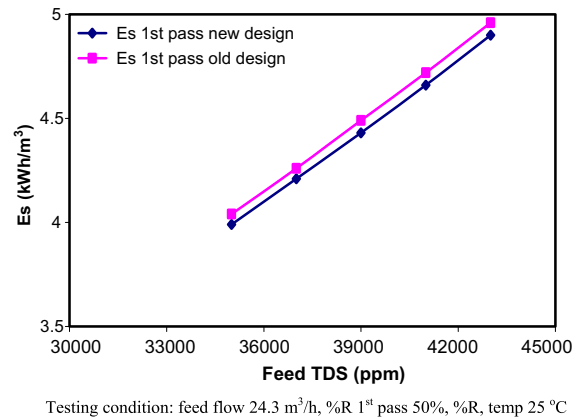


Fig. 17. Effect of feed salinity of 1st pass specific power consumption.

3% energy saving was achieved at feed temperature 15°C and dropped to 2.2% at 35°C. The permeate TDS from the conventional and new design were almost the same which means that there was no compromise in the permeate quality (Fig. 16).

As illustrated in Table 3, the applied feed pressure in the old design was higher than in the new design. This was probably due to the high membrane resistance in the old design. The structure of SW30HRLE-400i is tighter than SW30XLE-400i membrane, and

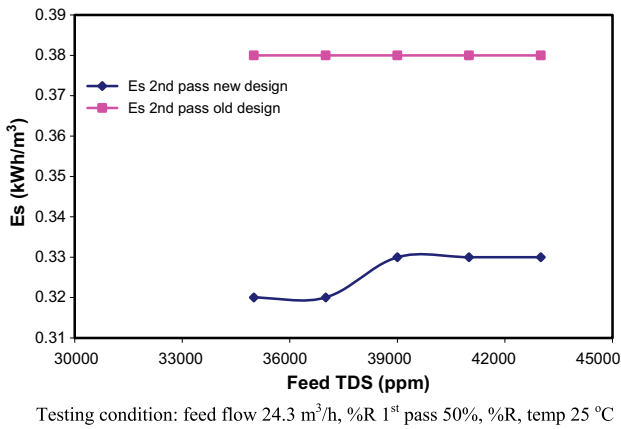


Fig. 18. Effect of feed salinity on 2nd pass specific power consumption.

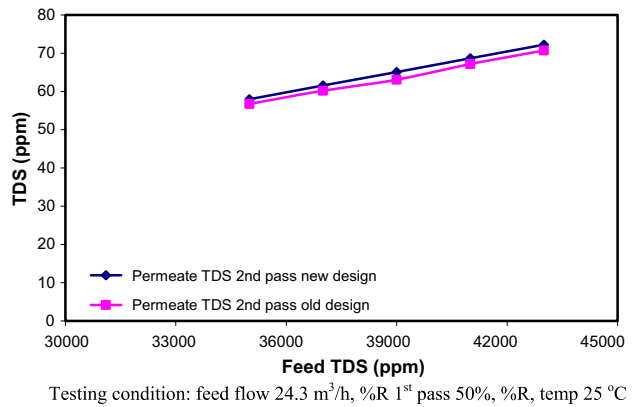


Fig. 21. Effect of feed salinity on 2nd pass permeate concentration.

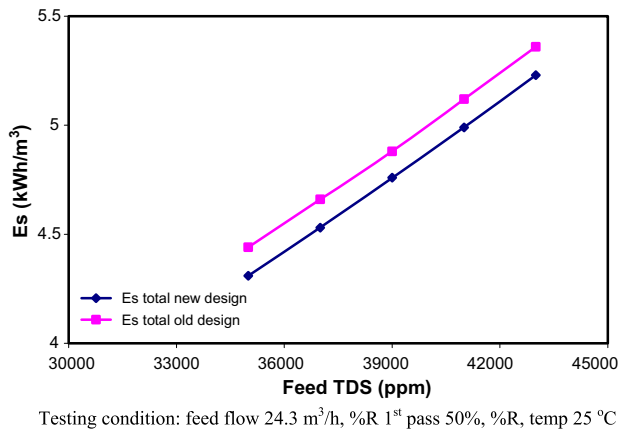


Fig. 19. Effect of feed salinity on total specific power consumption.

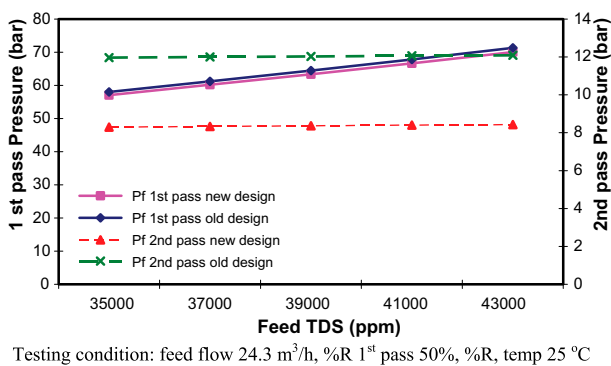


Fig. 20. Effect of feed salinity on feed pressure.

hence, a higher feed pressure was required for the seawater filtration. This was also substantiated by the

fact that the feed osmotic pressure in the old and new designs was almost equal (Table 3).

The new SWRO design was also tested for different salinities. A range of salinities from 35,000 to 43,000 ppm was investigated in this study. It was found that the energy requirements in pass 1 were lower in the new design. This trend was recorded for all feed salinities tested in this study (Fig. 17). This observation was also noticed in pass 2 BWRO membrane (Fig. 18). As a result, the total energy requirements for seawater desalination were higher in the old design compared with the new design (Fig. 19). The reason for this, as described earlier, was due to the tight structure of SWRO and BWRO membrane elements used in the old design. The total energy saving was 2.9% and 2.4% for the feed salinities 35,000 and 43,000 ppm, respectively. Finally, the feed pressure required for desalination in the old and new designs showed that a slightly higher pressure was required in the old design (Fig. 20).

In addition to its lower energy requirements, the concentration of permeate from the new design was equal to that from the old design. Permeate TDS in both designs was very close for all feed temperatures (Fig. 21). For large installation, the new design could be more efficient as the saving in energy will be more prominent.

### 6. Scale analysis

A scale analysis study was conducted on the new and conventional RO pressure vessel membrane arrangement design. Scaling is the precipitation and deposition of sparingly soluble salts, such as magnesium hydroxide, barium sulphate, calcium sulphate,

Table 4  
Testing conditions for convention and new RO pressure vessel design

SW TDS (mg/L <sup>a</sup> )	Element no.	RO element type	%R	Qf (m <sup>3</sup> /h)	Pf (bar)	Qp (m <sup>3</sup> /h)
35,000 (conven. design)	1	SW30-HRLE400i	15	4.2	46.19	0.62
	2	SW30-HRLE400i	12	3.58	46.1	0.45
	3	SW30-HRLE400i	10	3.13	46.02	0.3
	4	SW30-HRLE400i	7	2.83	45.96	0.2
	5	SW30-HRLE400i	5	2.63	45.9	0.13
	6	SW30-HRLE400i	3	2.5	4.85	0.09
	7	SW30-HRLE400i	3	2.42	4.8	0.06
	8	SW30-HRLE400i	2	2.36	45.75	0.05
35,000 (new design)	1	SW30-HRLE400i	15	4.2	45.76	0.61
	2	SW30-HRLE400i	12	3.59	45.66	0.44
	3	SW30-HRLE400i	10	3.15	45.59	0.3
	4	SW30-HRLE400i	7	2.85	45.52	0.2
	5	SW30-HRLE400i	5	2.65	45.46	0.13
	6	SW30XLE-400i	4	2.52	45.06	0.1
	7	SW30XLE-400i	3	2.43	45.01	0.07
	8	SW30XLE-400i	2	2.36	44.97	0.05
45,000 (conven. design)	1	SW30-HRLE400i	16	4.5	60.14	0.72
	2	SW30-HRLE400i	13	3.78	60.03	0.49
	3	SW30-HRLE400i	10	3.29	59.95	0.31
	4	SW30-HRLE400i	7	2.98	59.88	0.2
	5	SW30-HRLE400i	4	2.78	59.82	0.12
	6	SW30-HRLE400i	3	2.66	59.76	0.08
	7	SW30-HRLE400i	2	2.58	59.7	0.06
	8	SW30-HRLE400i	2	2.52	59.65	0.04
45,000 (new design)	1	SW30-HRLE400i	16	4.5	59.51	0.7
	2	SW30-HRLE400i	13	3.8	59.41	0.48
	3	SW30-HRLE400i	9	3.32	59.33	0.31
	4	SW30-HRLE400i	7	3	59.26	0.2
	5	SW30-HRLE400i	4	2.81	59.19	0.12
	6	SW30XLE-400i	3	2.68	58.79	0.09
	7	SW30XLE-400i	3	2.59	58.73	0.07
	8	SW30XLE-400i	2	2.53	58.68	0.05

<sup>a</sup>Feed temperature 25 °C.

strontium sulphate and calcium fluoride, when their concentrations exceed the solubility limits. The effect of feed salinity on the fouling of RO membrane was taken into account in this study; the operating conditions of RO membrane at different seawater TDS are listed in Table 4.

Seawater composition for 35,000 and 45,000 mg/L feed salinity is illustrated in Table 5 [25]. It is postulated that the scale potential increases with increasing the concentration of calcium and sulphate ions in the feed water. Scale potential also increases with increasing the membrane permeability due to the higher permeate flow rate which results in brine concentrate of high TDS. A membrane with a high salt rejection rate and/or permeability tended to be more susceptible to scale fouling than a membrane with a low salt rejection and permeability.

Table 5  
Seawater composition at different feed salinity

Ions	35,000 (mg/L)	45,000 (mg/L)
K	380	496
Na	10,865	13,817
Mg	1,290	1,657
Ca	412	539
Sr	13	13
Ba	0.05	0.05
HCO <sub>3</sub>	142	182
Cl	19,500	24,868
F	1.3	1.3
SO <sub>4</sub>	2,712	3,472
SiO <sub>2</sub>	4.28	4.28
B	4	4

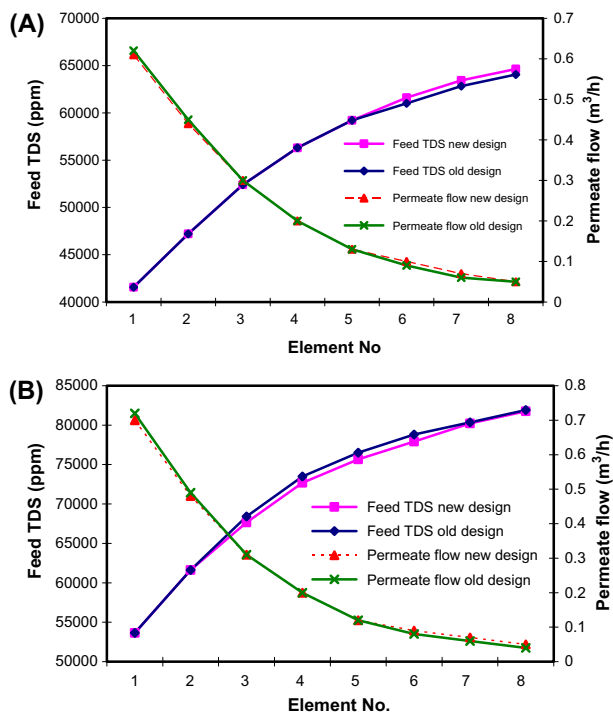


Fig. 22. Feed TDS and permeate flow for each element in the pressure vessel. (A) initial feed TDS 35,000 mg/L and (B) initial feed TDS 45,000 mg/L.

In the pressure vessel, the concentrate from first element is the feed to the subsequent element. Fig. 22 shows the profile of feed concentration and the permeate flow rate for each elements in the pressure vessel for 35,000 and 45,000 mg/L feed salinities. The concentration of feed water increased from the first to the last element, while permeate flow rate decreased due to the osmotic pressure increase.

At 35,000 mg/L feed salinity results from ROSA simulation program showed that the scale potential due to SrSO<sub>4</sub> in the new pressure vessel design was higher than in the conventional design (Fig. 23(A)). This was particularly evident in the last three tail elements in the new pressure vessel design. This was probably attributed to the higher feed concentration to the tail elements in the new design as illustrated in Fig. 22(A). These results demonstrate that the new design was less effective in reducing fouling potential in the RO membrane, although it was more economic in terms of power consumption.

At higher feed salinity, 45,000 mg/L, the profile of scale potential due to SrSO<sub>4</sub> was slightly different to that at feed salinity 35,000 mg/L (Fig. 23(B)). The reason for that was probably due to the variation in the recovery rate throughout the pressure vessel which in turn affected the permeate flow and feed TDS

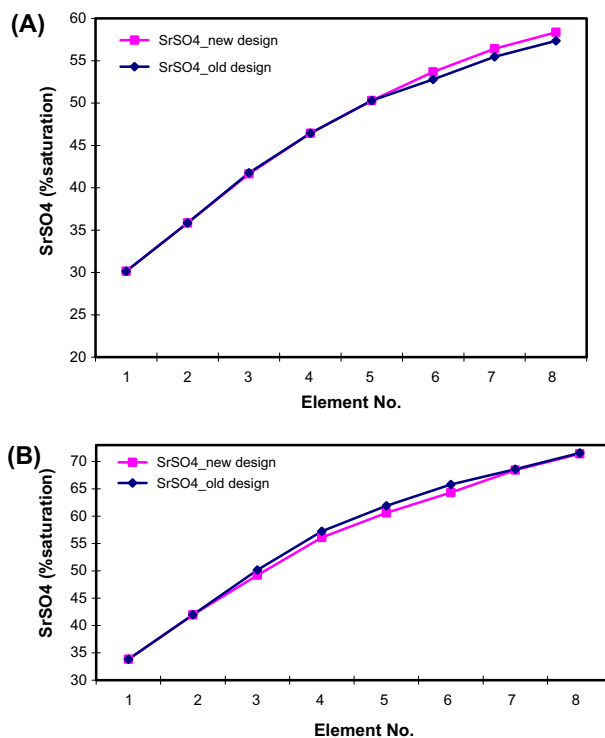


Fig. 23. SrSO<sub>4</sub> scale in the RO membrane elements at different feed salinity. (A) 35,000 mg/L and (B) 45,000 mg/L.

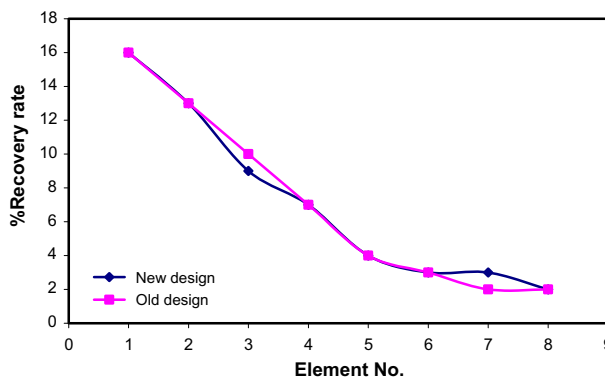


Fig. 24. Recovery rate throughout the pressure vessel.

(Fig. 24). As shown in Fig. 24, the recovery rate in the new design at element three was lower than in the old design, equalized at elements five and six, then increased at element seven and finally equalized at element eight. The concentration of feed salinity and permeate flow rate in the new design is illustrated in Fig. 22(B). Feed TDS of RO elements three to eight was higher in the old design than in the new design. Meanwhile, the permeate flow in the front elements one and two was higher in the old design than in the new design, but this trend was reversed towards the

Table 6  
Annual energy cost for desalination

Salinity (mg/L)	Conventional design cost (\$/year)	New design cost (\$/year)	Difference (conventional-new) (\$/year)
35,000	8,103,000	7,865,750	237,250
37,000	8,504,500	8,267,250	237,250
39,000	8,906,000	8,687,000	219,000
41,000	9,344,000	9,106,750	237,250
43,000	9,782,000	9,544,750	237,250
45,000	10,256,500	9,982,750	273,750

tails elements six to eight, and it was lower in the old design than in the new design. It should be noted here that Strontium scale always affects the back-end of the RO element, and its solubility decreases with increasing the concentration of sulphate in solution [24] which was the usual case in the tail RO elements. Interestingly, the simulation results showed that the  $\text{SrSO}_4$  scaling is independent of the solution pH [24].

In brief, the results from ROSA showed that at feed TDS, 35,000 mg/L, the new design was prone to scale fouling more than the old design; especially sulphate and fluoride scales. To overcome this problem, antiscalant needs to be dosed into the feed stream. Although the new design was more energy efficient at 35,000 mg/L feed salinity, the scale propensity was higher than in the old design. But at feed salinity, 45,000 mg/L, the new design worked more efficiently than the old design in terms of scale fouling and power consumption. Therefore, the concentration of seawater should be taken into account when implementing the new design.

## 7. Energy cost

In this study, the cost of energy was estimated to be USD 0.05 \$/kWh. The specific power consumption for feed salinity range from 35,000 to 45,000 mg/L, plant capacity 100,000 m<sup>3</sup>/day, is calculated from the following equation:

$$\text{Energy cost} = \text{Plant capacity (m}^3/\text{d)} \times \text{energy cost} \\ (\text{/kWh}) \times \text{time (days)} \times \text{Es (kWh/m}^3)$$

The energy costs of the conventional and new RO designs are listed in Table 6.

According to the results in Table 6, it seems that the new design was more efficient than the old design. These results are illustrated in Fig. 25.

## 8. Conclusion

Two different designs were proposed in this study. In the first design, SWRO and BWRO elements of similar type were conventionally loaded in the pressure vessel, while in the second design, two different types of SWRO and BWRO elements were packed in the pressure vessel. The results from ROSA showed that the latter design slightly outperformed the conventional design in terms of energy consumption without compromising the permeate quality. The number and position of high-permeability SWRO and BWRO was carefully optimized to achieve the optimal performance. After optimization, the energy consumption was calculated for each design, and the results showed a subtle advantage in favour of the new design. The economic benefits of the new design can be realized more evidently in large RO seawater desalination as the operation cost increases with increasing the plant capacity.

Additionally, a scale analysis study was conducted to investigate the effect of new membrane arrangement design on the membrane fouling. Scale problems have adverse impacts on the membrane performance in short and long term. In short term, it will increase the use of antiscalants in the seawater feed to RO, and the membrane performance will be deteriorated in long term [25]. However, it was found that the scale potential was sensitive to feed salinity. At feed salinity 35,000 mg/L, the scale potential was higher in the new design compared with the old design. This trend was reversed at feed salinity 45,000 mg/L as the scale potential was lower in the new design than in the old design.

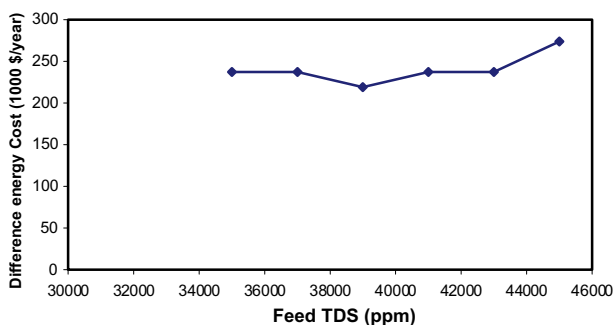


Fig. 25. Energy cost difference between new and old RO pressure vessel design.

In commercial applications, the proposed design approach here can be applied to any type of membranes and manufacturing companies. The design approach is not strictly applicable for two type membranes; more than two types of membrane elements could also be used in the pressure vessel to enhance the performance in terms of power consumption and reducing scale problems. Pilot plant studies may be required for optimization purpose before commercialization.

## References

- [1] N. Hilal, H. Al-Zoubi, N.A. Darwish, A.W. Mohamma, M. Abu Arabi, A comprehensive review of nanofiltration membranes: Treatment, pretreatment, modelling, and atomic force microscopy, *Desalination* 170 (2004) 281–308
- [2] E. El-Zanati, K.M. El-Khatib, Integrated membrane-based desalination system, *Desalination* 205 (2007) 15–25
- [3] A. Sánchez Sánchez, J.M. Garrido, R. Méndez, A comparative study of tertiary membrane filtration of industrial wastewater treated in a granular and a flocculent sludge SBR, *Desalination* 250 (2010) 810–814.
- [4] K. Biswas, K. Gupta, A. Goswami, U. Ghosh, Fluoride removal efficiency from aqueous solution by synthetic iron(III)–aluminum(III)–chromium(III) ternary mixed oxide, *Desalination* 255 (2010) 44–51.
- [5] S.A. Avlonitis, Operational water cost and productivity improvements for small-size RO desalination plants, *Desalination* 142 (2002) 295–304.
- [6] C. Fritzmann, J. Löwenberg, T. Wintgens, T. Melin, State-of-the-art of reverse osmosis desalination, *Desalination* 216 (2007) 1–76.
- [7] I.C. Karagiannis, P.G. Soldatos, Water desalination cost literature: Review and assessment, *Desalination* 223 (2008) 448–456.
- [8] R. Borsani, S. Rebagliati, Fundamentals and costing of MSF desalination plants and comparison with other technologies, *Desalination* 182 (2005) 29–37.
- [9] M. Bessenasse, A. Kettab, Adnane Souffi Moulla, Sea-water desalination: Study of three coastal stations in Algiers region, *Desalination* 250 (2010) 423–427.
- [10] K. Quteishat, M.K. Abu Arabi, K.V. Reddy, Review of MEDRC R&D projects, *Desalination* 156 (2003) 1–20.
- [11] O.A. Hamed, Overview of hybrid desalination systems—Current status and future prospects, *Desalination* 186 (2005) 207–214.
- [12] M.A.K. Abdul-Kareem Al-Sofi, Seawater desalination—SWCC experience and vision, *Desalination* 135 (2001) 121–139.
- [13] M. Abdel-Jawad, E.E.F. El-Sayed, S. Ebrahim, A. Al-Saffar, M. Safar, M. Tabtabaei, G. Al-Nuwaibit, Fifteen years of R&D program in seawater desalination at KISR part II. RO system performance, *Desalination* 135 (2001) 155–167.
- [14] I. El Saliby, Y. Okour, H.K. Shon, J. Kandasamy, Desalination plants in Australia, review and facts, *Desalination* 247 (2009) 1–14.
- [15] K. Chinu, A.H. Johir, S. Vigneswaran, H.K. Shon, Jaya Kandasamy, Assessment of pretreatment to microfiltration for desalination in terms of fouling index and molecular weight distribution, *Desalination* 250 (2010) 644–647.
- [16] N. Prihasto, Q.-F. Liu, S.-H. Kim, Pre-treatment strategies for seawater desalination by reverse osmosis system, *Desalination* 249 (2009) 308–316.
- [17] S.S. Mitra, A.R. Thomas, G.T. Gang, Evaluation and characterization of seawater RO membrane fouling, *Desalination* 247 (2009) 94–107.
- [18] P. Palomar, I.J. Losada, Desalination in Spain: Recent developments and recommendations, *Desalination* 255 (2010) 97–106.
- [19] A.M. Hassan, A.M. Farooque, A.T.M. Jamaluddin, A.S. Al-Amoudi, M.A.K. Al-Sofi, A.F. Al-Rubaian, N.M. Kither, I.A.R. Al-Tisan, A. Rowaili, A demonstration plant based on the new NF-SWRO process, *Desalination* 131 (2000) 157–171.
- [20] A. Zach-Maor, R. Semiat, A. Rahardianto, Y. Cohen, S. Wilson, S.R. Gray, Diagnostic analysis of RO desalting treated wastewater, *Desalination* 230 (2008) 239–247.
- [21] H.Y. Ng, K.G. Tay, S.C. Chua, H. Seah, Novel 16-inch spiral-wound RO systems for water reclamation—A quantum leap in water reclamation technology, *Desalination* 225 (2008) 274–287.
- [22] F. Vince, F. Marechal, E. Aoustin, P. Bréant, Multi-objective optimization of RO desalination plants, *Desalination* 222 (2008) 96–118.
- [23] M. Wilf, K. Klinko, Optimization of seawater RO system design, *Hydranautics*, Available from [www.membrane.com](http://www.membrane.com) (accessed 21 December 2009).
- [24] Feed water type and analysis, Tech Manual Excerpt, Available from [http://www.dow.com/PublishedLiterature/dh\\_003b/0901b8038003b4a0.pdf?filepath=liquidseps/pdfs/noreg/609-02010.pdf&fromPage=GetDoc](http://www.dow.com/PublishedLiterature/dh_003b/0901b8038003b4a0.pdf?filepath=liquidseps/pdfs/noreg/609-02010.pdf&fromPage=GetDoc) (accessed 14 September 2010).
- [25] Reverse Osmosis Water Chemistry, *Hydranautics*, Available from [http://www.membranes.com/docs/papers/04\\_ro\\_water\\_chemistry.pdf](http://www.membranes.com/docs/papers/04_ro_water_chemistry.pdf) (accessed 11 September 2013).